Processes controlling the dynamics of compound sand waves in the North Sea, Netherlands

Thaiënne A. G. P. van Dijk
Netherlands Institute of Applied Geosciences, Utrecht, Netherlands

Maarten G. Kleinhans
Department of Physical Geography, Institute of Marine and Atmospheric Research, University of Utrecht, Utrecht, Netherlands

Received 1 June 2004; revised 23 January 2005; accepted 21 February 2005; published 3 November 2005.

[1] The understanding of the morphodynamics of harmonic bed forms on the seabed is essential for modeling marine sediment transport and coastal morphologic development. Previous research has mainly focused on the type and distribution of bed forms, but areally extensive data and time series of seabed features are scarce. Multibeam and side-scan sonar data from four expeditions reveal the contrasts between a coastal site with asymmetric and flattened, three-dimensional (3-D) compound sand waves on a shoreface-connected ridge and an offshore site with asymmetric and sharp-crested, 2-D compound sand waves. Migration rates of the coastal sand waves are 6.5–20 m yr^{-1}, while migration rates of the offshore sand waves are −3.6 to 10 m yr^{-1}. This contrasting morphology and dynamic behavior of compound sand waves at the two North Sea sites is explained by differences in the relative importance of tidal currents and wave activity near the bed. These new field data provide parameters and boundary conditions for sand transport models, while the empirically derived behavior of sand waves may be used to validate sand transport and sand wave models.

Citation: van Dijk, T. A. G. P., and M. G. Kleinhans (2005), Processes controlling the dynamics of compound sand waves in the North Sea, Netherlands, *J. Geophys. Res.*, *110*, F04S10, doi:10.1029/2004JF000173.

1. Introduction

[2] Harmonic bed forms of a wide range of scales characterize the shallow parts of most sandy continental shelves. For the North Sea, bed forms were mapped by *Van Alphen and Damoiseaux* [1989], and the occurrence of sand waves specifically was later successfully predicted by *Hulscher and Van den Brink* [2001]. These harmonic bed forms are important seabed features, for example, for explaining their morphologic effect on benthic habitats (e.g. M. J. Baptist et al., The distribution of macrozoobenthos in the southern North Sea in relation to small-scale morphological features, submitted to *Estuarine and Coastal Shelf Science*, 2005) and as dynamic elements, for example, for predicting seabed changes, coastline development and the effects of man-made structures. Compound sand waves, which are the subject of this paper, are defined as flow-transverse marine subaqueous dunes with superimposed megaripples and have a typical length of 100 to 800 m and heights of several meters [e.g., *Terwindt*, 1971; *Tobias*, 1989; *Van Alphen and Damoiseaux*, 1989; *Ashley*, 1990; *Besio et al.*, 2004]. Slope angles of both the stoss and lee slopes of sand waves are very small (less than 10°); thus lee slopes do not resemble slip faces. The superimposed megaripples are flow-transverse bed forms with a typical length of 5 to 20 m and heights of 0.2 to 1.5 m [e.g., *Tobias*, 1989; *Ashley*, 1990].

[3] *Hulscher* [1996] demonstrated in a three-dimensional morphodynamic model, using linear stability analysis, that sand waves are generated by the residual vertical circulation caused by the interaction of oscillatory tidal flow and bed perturbations, whereby their growth is realized by the convergence of sediment from the troughs to the crests. Field observations that megaripples are directed toward sand wave crests support this finding [e.g., *Terwindt*, 1971]. *Komarova and Hulscher* [2000] improved this model into a sophisticated turbulence model, which allows for a variable thickness of the current boundary layer due to a changing bed roughness during the morphodynamic loop. The modeled variation in the boundary layer thickness over sand waves and the bed roughness affect the bed shear stress and hence the sediment transport [*Soulsby*, 1997; *Idier et al.*, 2004].

[4] Recently extended morphodynamic models evince that sand waves migrate due to an asymmetry in the vertical circulative water motion induced by the interaction of a steady current (*Z*0) or higher-frequency tidal constituents (e.g., *M*4) with the symmetrical main tidal motion (*M*2) [*Németh et al.*, 2002; *Besio et al.*, 2003]. *Németh et al.*'s [2002] 2-D vertical model excludes the second horizontal

0148-0227/05/2004JF000173

direction and higher-frequency tidal constituents and results in a migration of sand waves which is normal to the sand wave crests and always in the direction of the residual flow. However, field observations show that sand wave crests may shift both in and against the direction of the residual current [*Lanckneus and De Moor*, 1991; *Besio et al.*, 2004]. Our field observations presented in this paper confirm this finding. *Besio et al.* [2003, 2004] recently demonstrated that although both the residual current $Z0$ and higher-frequency tidal constituent $M4$ may cause sand wave migration, it is the harmonic constituent $M4$ that may cause sand wave migration in the direction against the residual flow.

[5] Present-day sand wave evolution models assume that bed load transport is the only sediment transport mechanism, whilst for instance *Flemming* [2000] explains the saturation of sand waves with suspended load transport. Furthermore, the forcing of surface waves is thought to be an important mechanism that affects the shape and dynamics of both small- and large-scaled bed forms [e.g., *Tobias*, 1989; *Blondeaux and Vittori*, 1999; *Calvete et al.*, 2002; *Idier and Astruc*, 2003; *Idier et al.*, 2004]. *Blondeaux et al.*'s [2000] 3-D model for sand wave generation and evolution includes the forcing by surface waves and suspended sediment transport. The model of *Calvete et al.* [2002] shows that suspended load flux and wave stirring shorten saturation times of larger-scaled shoreface-connected ridges considerably, resulting in realistic migration speeds of the ridges. However, the explicit impact of these mechanisms on sand wave migration remains to be explained.

[6] The validity of models that describe the evolution and behavior of sand waves can be evaluated by the comparison of model results to field data. Since the horizontal positioning error from older field data exceeds the migration rates of sand waves [e.g., *Terwindt*, 1971], there is a need for modern and accurate field data of the characteristics of sand waves, as recently called for by *Németh et al.* [2002] and *Németh* [2003]. The necessity for more field measurements for testing sediment transport models was also identified by *Davies et al.* [2002], who state that model outputs of total sediment transport from various sediment transport models may vary up to several orders of magnitude with field data. Predictions are poorer for rippled beds with high surface roughness coefficients and long-term dynamics are poorly understood due to the scarcity of time series of field data.

[7] In this paper we present new time series of accurate and full coverage imagery of two North Sea sites with compound sand waves several km^2 in size, of in total utilizing five expeditions over a period of 1.5 years, in order to derive migration rates of sand waves. In this study we aim to identify and explain the processes that control the morphology and dynamic behavior of these bed forms under the hydrodynamic conditions of the North Sea. We hereto demonstrate the relative importance of currents and surface waves on the sand wave morphology and dynamics by calculating the realistic impact of currents and surface waves on the bed, thereby supporting the interpretation of our field observations. We focus on compound sand waves and not on tidal banks [e.g., *Van de Meene*, 1994] or short-lived hummocky morphology (S. Passchier and M. G. Kleinhans, Observations of megaripples and hummocky cross-stratification in the Dutch coastal area and their relation to currents and combined flow conditions, submitted to *Journal of Geophysical Research*, 2004 hereinafter referred to as Passchier and Kleinhans, submitted manuscript, 2004). Since the superimposed megaripples adapt more rapidly to changes in conditions than sand waves, for example opposing directions due to the tide [*Lanckneus and De Moor*, 1991] or storm-related obliteration [*Houthuys et al.*, 1994] and rapid generation, megaripples are used as dynamic indicators for processes that control the behavior of compound sand waves.

2. Methods

[8] Morphologic and morphodynamic data are compared from two of our survey sites in the North Sea. The first site is a coastal site (1770 × 1625 m) in an area with shoreface-connected ridges [*Van Alphen and Damoiseaux*, 1989; *Van de Meene*, 1994] and water depths of 14–18 m, 6–8 km west of Zandvoort (Figure 1). The second site is an offshore site (5510 × 1100 m) in a sand wave field [*Van Alphen and Damoiseaux*, 1989] at 27–30 m water depths, 50 km west of Egmond aan Zee (Figure 1). Areally extensive morphology of the seabed was imaged with a hull-mounted SIMRAD ED3000 D multibeam echo sounder and a shallowly towed Dowty 310 side-scan sonar. The multibeam operates at a frequency of 300 kHz and the sonar at 325 kHz. Data were acquired on 4 expeditions in March, June/July and September/October 2001 and April 2002, and for the offshore site also in September 2002. The multibeam data were corrected for tidal water level fluctuations using two permanent stations at IJmuiden and Noordwijk and two MORS tide gauges at buoy MO12 for the offshore site and the Eveline buoy for the coastal site. The horizontal positioning system was a dGPS with an accuracy of 1 m.

[9] During the above 4 expeditions, the seabed was sampled using a cylindrical box corer with a diameter of 32 cm, from which cores of 10 cm diameter were resampled. We sampled on stoss slopes, crests and in troughs of sand waves both on the ridge and in the swale at the coastal site and at similar morphologic elements of two sand waves in the southern part of the offshore site. We used the same locations each expedition, to a total number of samples per expedition varying between 13 and 17 at the coastal site and 12 and 19 at the offshore site. Grain size samples for grains <2 mm were analyzed by laser diffraction, using a Malvern 2000.

[10] Lengths and heights of bed forms were measured manually from the corrected multibeam images, which were plotted at scale 1:2500, and from bathymetric profiles normal to the sand wave crests, which were compiled from the multibeam data and plotted at a horizontal scale of 1:2500 and a vertical scale of 1:25. Wavelengths of megaripples were determined as an average of 7–10 adjacent megaripples. Morphodynamics of compound sand waves were investigated both in plan view and in cross-sectional profile. The comparison of profiles of different data sets over time provides the migration rates of the sand waves, also measured manually with a linear scale. Hereby, migration rates were measured on lee slopes rather than at the

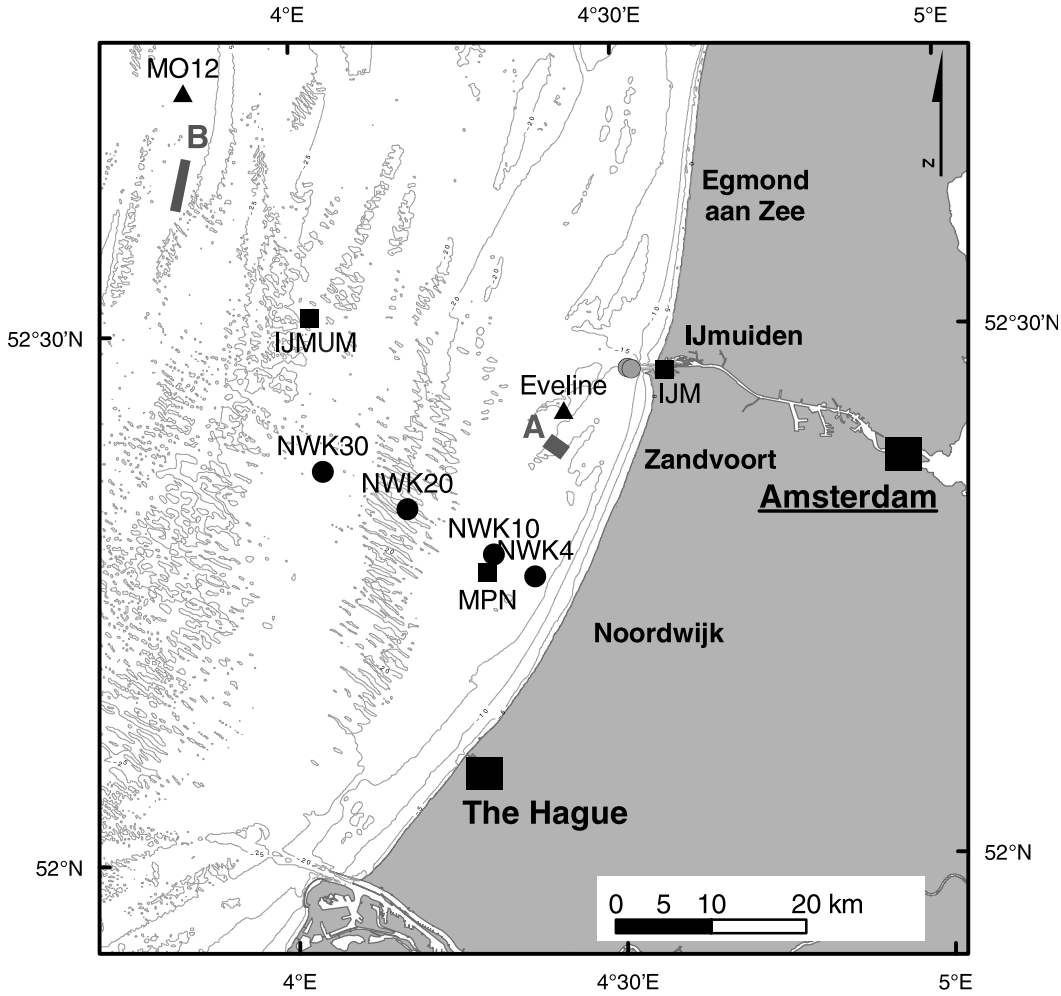

Figure 1. Bathymetry map of the North Sea near IJmuiden, Netherlands, indicating the location of the coastal site (A) in the shoreface-connected ridge area and the offshore site (B) in a sand wave field. Monitoring stations and tide gauges are indicated: MPN, monitoring station Noordwijk; IJM, monitoring station IJmuiden; IJMUN, IJmuiden Munition Dump; NWK4, NWK10, NWK20, NWK30, Noordwijk 4, 10, 20, and 30 km offshore, respectively; Eveline and MO12, buoys with tide gauges.

crests of sand waves, because the crest variability due to megaripple variation is larger than that due to sand wave displacement. In the coastal area, the migration is relatively uniform for the entire lee slopes. In the offshore area, profiles of two subsequent surveys show that lee slopes of sand waves commonly intersect at a point approximately half way down slope (Figure 2). Therefore migration rates of sand waves at the offshore site were measured separately for the upper and lower lee slopes (Figure 2). Profiles do not run over bifurcations but do include bifurcated sand waves, which were measured individually (they are plotted at the same sand wave number on the x axes of Figures 6 and 7). In order to produce comparable migration rates, measured migration rates of the coastal site were extrapolated to annual migration rates and those of the offshore site were reduced to annual rates. This is justified because this paper concludes that sand wave migration in the coastal area is due to continuous wave stirring and current action rather than event-controlled migration. Migration rates of megaripples were not established, since individual megaripples

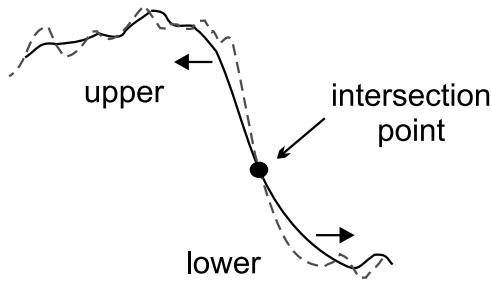

Figure 2. Definition of the upper and lower lee slopes as separated by the point on the lee slope where subsequent profiles intersect. Upper lee slopes commonly move against the residual flow direction, whereas lower lee slopes commonly move down flow. The height of the intersection points may vary slightly per sand wave.

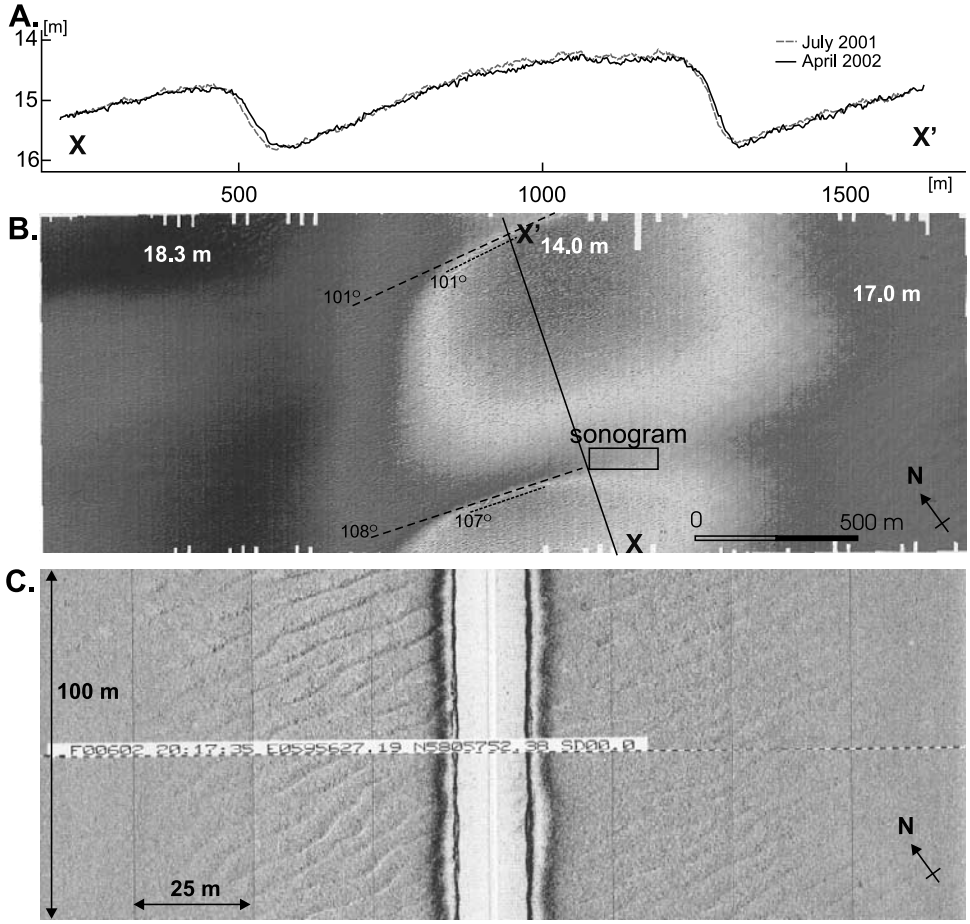

Figure 3. Morphology of the coastal site. (a) bathymetry of July 2001 and April 2002, (b) multibeam image with crest orientations of sand waves and megaripples, water depths, locations of bathymetry profiles, and the sonogram, and (c) uncorrected side-scan sonar image of the box in Figure 3b. The sailing course was 36° (from bottom to top). See color version of this figure in the HTML.

that were identified in one season could not be identified on the images and profiles of the following season.

[11] Wave and current parameters used in descriptions and calculations are (averaged) measured values from data sets at several monitoring stations of National Survey Institutes (Figure 1).

3. Results

[12] All morphologic descriptions in this section are observations made in March 2001, after a 3 month period of fair weather conditions (http://www.weeronline.nl and http://www.knmi.nl) and one month into a 2.5 month period during which the sites were closed to beam trawl fishing. Because the large-scaled morphology of the sites and the orientation of sand waves and megaripples remain relatively similar over time, we chose not to describe the morphology of all four surveys individually. The results of the four expeditions will be mainly used for the morphodynamic descriptions.

3.1. Coastal Shoreface-Connected Ridge Site

[13] Multibeam images and profiles of the seabed in the coastal area reveal a shoreface-connected ridge with superimposed compound sand waves (Figure 3b). These sand waves are three-dimensional in form and strongly asymmetric in cross section (Table 1) with their lee sides facing north-northeast. The length of the northern sand wave is 760 m and the height difference between the flat-topped crest plateau and the adjacent trough is 1.5 m. The orientation of the axis of the ridge is 36° from UTM north; the orientations of the sand wave crests are 101° and 108° from UTM north. The respective orientations of megaripples near the sand wave crests are 101° and 107° from UTM north and thus perfectly parallel to the sand wave crests. Megaripple orientations on the stoss side of both sand waves are 103° from UTM north. Megaripples have two-dimensional sinuous crests and are asymmetric in cross section, with their steep sides facing north. Their average length in March 2001 is 6.6 m. Although the megaripples are approximately uniform, their appearance on the sonograms changes over the lengths of sand waves. Megaripples in the sand wave troughs are coarse-pixeled and are characterized by both high- (dark) and low-backscatter (light) intensities, whereas megaripples on the stoss slopes and lower crest plateaus appear smoother and are merely highlighted with low-backscatter intensities (light-colored acoustical shadows) (Figure 3c).

[14] Megaripples were by far the best developed in March 2001. In June/July 2001, the distinct megaripples had faded

Table 1. Statistics of the Bed Form Morphology, Dynamics, and Grain Size at Two Sites in the North Sea

	Coastal Site		Offshore Site (Averages)	
	Sand Waves	Megaripples	Sand Waves	Megaripples
Wavelength L, m	760	6.6	203	10.14
Wave height H, m	1.5	0.05–0.10	1.79	<0.40
Dune index L/H	507	132–66	126	>25
Crest orientation (from UTM north)	101° and 108°	101° and 107° (103° on stoss)	91°	121° (136° in troughs; 110° near crests)
Symmetry index L_{stoss}/L_{lee}	10.7	-	4.23	-
Gradient stoss side	0.20°	-	0.66°	-
Gradient lee side	1.11°	-	2.34°	-
Migration rate, m yr^{-1}	6.5–20	-	−3.4–10.2	-
	Coastal Site		Offshore Site	
Water depth, m	14–18.3		26–30	
Grain size, all voyages, μm				
D_{50} range (average)	279–366 (326)		254–304 (278)	
D_{10} range (average)	188–263 (230)		178–219 (198)	
D_{90} range (average)	414–510 (463)		364–423 (389)	

either completely, to a merely grainy structure on the sonograms, or to a barely recognizable lineation, apart from a zone of distinct ripples limited to the seaward flank of the shoreface-connected ridge. In October 2001 all megaripples were obliterated.

[15] The comparison of the July 2001 and April 2002 profiles of the coastal area demonstrates a northward migration of the sand waves (Figure 3a). The minimum and maximum horizontal displacement of the lee side of the southern sand wave was 7.5–12.5 m, that of the trough between the sand waves 15.0 m, that of the lee side of the northern sand wave 5.0–7.5 m and of the trough on the north side 5.0 m, which are significant with a horizontal error of 1 m. These values correspond to a migration rate of 6.5–20 m yr^{-1}. Detailed profiles over shorter time intervals, however, show a contrasting behavior of the lee slope. Between the profiles of March and June 2001, the lee slope location remains nearly unchanged, the June and September 2001 profiles show a southward displacement of maximal 4.3 m and those of September 2001 and April 2002 show a northward displacement of maximal 10 m (Figure 4). Our measurements agree well to those reported in the literature of other North Sea sites. *Lanckneus and De Moor* [1991] reported temporal horizontal displacements of sand waves in opposite directions on the Belgium continental shelf. The displacement rates that we determined at the coastal site are smaller than those of *Lanckneus and De Moor* [1991], who found an average of 28 m westward in a 4 month period (February to June 1989) and 29 m to east in a 5 month period (June to November 1989). Our data also agree well with measurements of *Besio et al.* [2004], who find average migration rates from 1.5 to 6.0 m yr^{-1} in the direction of the

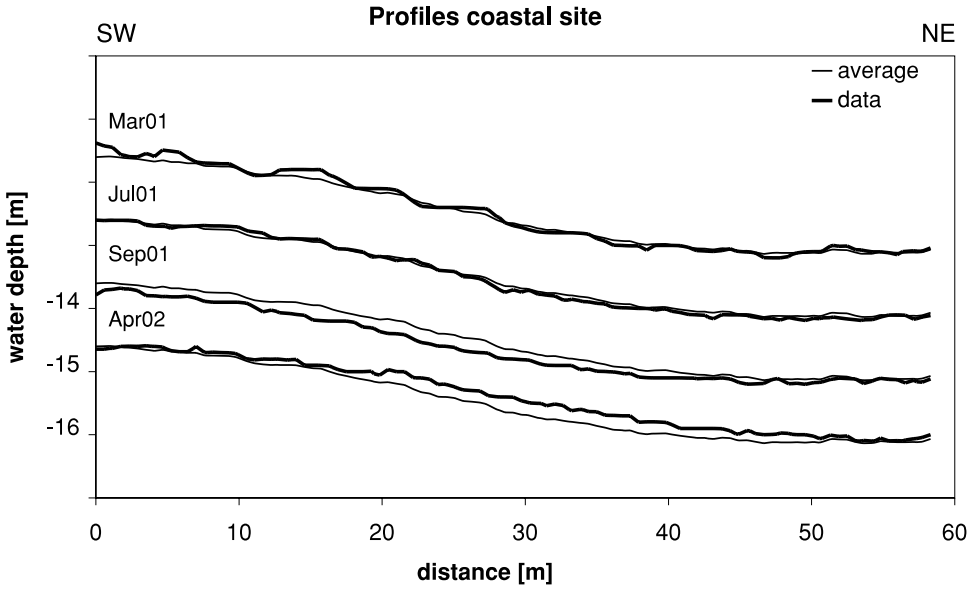

Figure 4. Detailed profiles (from SW to NE) of the lee slope of the southern sand wave of four surveys at the coastal site. For clarity, the profiles are plotted separately, each with a +1 m offset. Only the profile of April 2002 is plotted at real water depths. The averaged profile (thin shaded line) plotted with each measured data profile (solid line) allows for the comparison between the four data profiles. The profiles show very small southward migration between March 2001 and July 2001, greater southward migration between July and September 2001, and even greater but northward migration between September 2001 and April 2002.

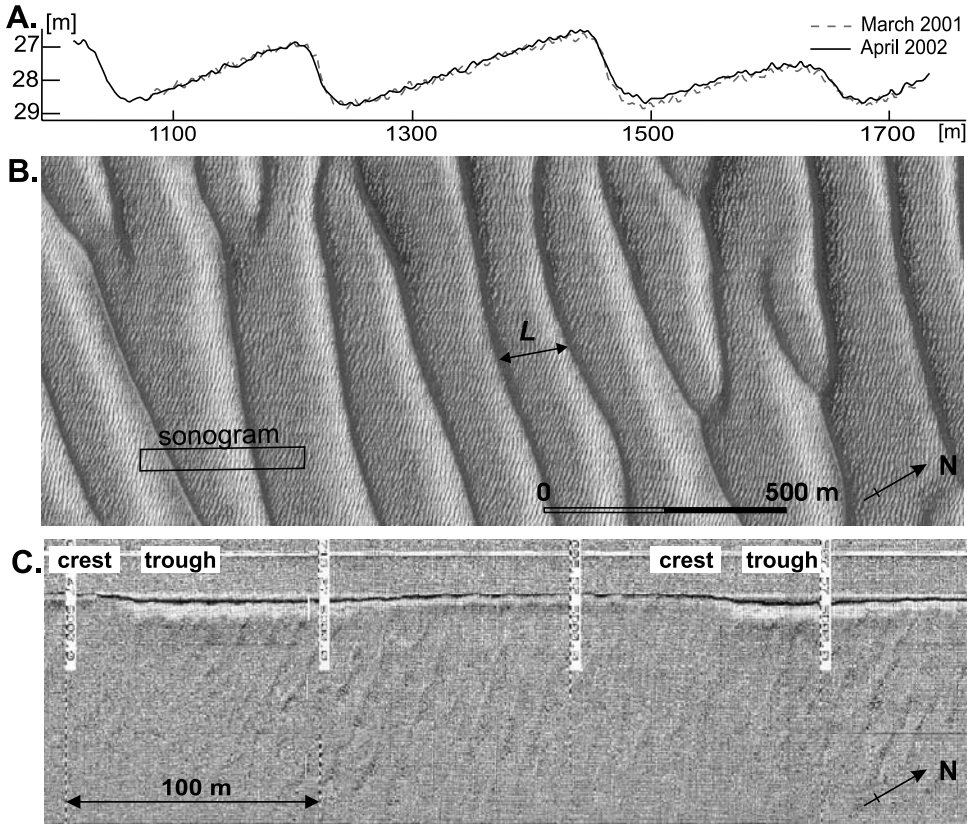

Figure 5. Morphology of the offshore site. (a) Bathymetry of March 2001 and April 2002 (southern part of the area, off the image in Figure 5b). (b) Multibeam image. (c) Uncorrected side-scan sonar image of the box in Figure 5b. The visible slant range is 75 m, the distance between two white lines is ~100 m, and the sailing course was 30° (from left to right). See color version of this figure in the HTML.

residual flow at an offshore site and 3.5–8.8 m yr^{-1} against the residual flow at a coastal site near the Belgian shore.

[16] Seabed sediments in the coastal area are moderately sorted, fine to coarse sands with grain sizes ranging between 150 and 900 μm and sample medians, D_{50}, ranging between 280 and 366 μm (Table 1). Grains finer than 63 μm do not occur in the surface samples. A fining trend in sample medians perpendicular away from the shore is dominant over grain size variations correlated to the ridge and sand wave morphology, which is consistent with earlier findings of *Van de Meene et al.* [1996] but in contrast with the trend observed by *Trentesaux et al.* [1994], who found coarser and poorer sorted sediments on a Flemish tidal bank. Although the morphology-related grain size differences are subordinate, clustering of samples per morphological unit in bivariate plots of sorting against median is recognizable (see Passchier and Kleinhans, submitted manuscript, 2004, Figure 6). Differences between medians of sand wave crests and troughs are small, on average 24 μm coarser at the crests, but nonetheless occur at both sand waves in all seasons. The average maximum seasonal variation in grain size median per sample location is less than 20 μm. Repetitive analyses have shown that the sampling error is ~20 μm.

3.2. Offshore Sand Wave Field

[17] The seabed morphology in the offshore area comprises nearly two-dimensional compound sand waves (Figure 5b). In cross-sectional profile, the sand waves are asymmetric, though less asymmetric than those in the coastal area (Table 1) with their lee slopes facing north. Most sand waves are sharp crested, but few are rounded (Figure 5a). The average wavelength of the sand waves is 203 m and the average wave height is 1.79 m. Although some sand waves display open or buttress junctions, the sand wave crests are straight to sinuous and very continuous when compared to sand waves that occur just to the south of our site [see *Besio et al.*, 2004].

[18] The average orientation of the crests is 91° from UTM north. The average crest orientation of the superimposed asymmetric megaripples is 121° from UTM north, which thus makes an angle of 30° with the average crest orientation of the sand waves. The orientations of megaripples systematically vary over the lengths of sand waves, with orientations of 136.5° in the troughs, 116.6° on the stoss sides and 110.6° near the crests (Figure 6). Near sand wave crests, the angle between crest orientations of sand waves and megaripples is thus 19.6°. This corresponds well to the orientation angles between sand wave crests and megaripple crests reported in the literature [e.g., *Terwindt*, 1971; *Malikides et al.*, 1989; *Lanckneus and De Moor*, 1991; *Hennings et al.*, 2000].

[19] On the sonograms, a repetitive and systematic pattern of variable forms and appearances of megaripples, similar to the variable appearance in the coastal site, corresponds to the morphologic elements of sand waves (Figure 5). In sand

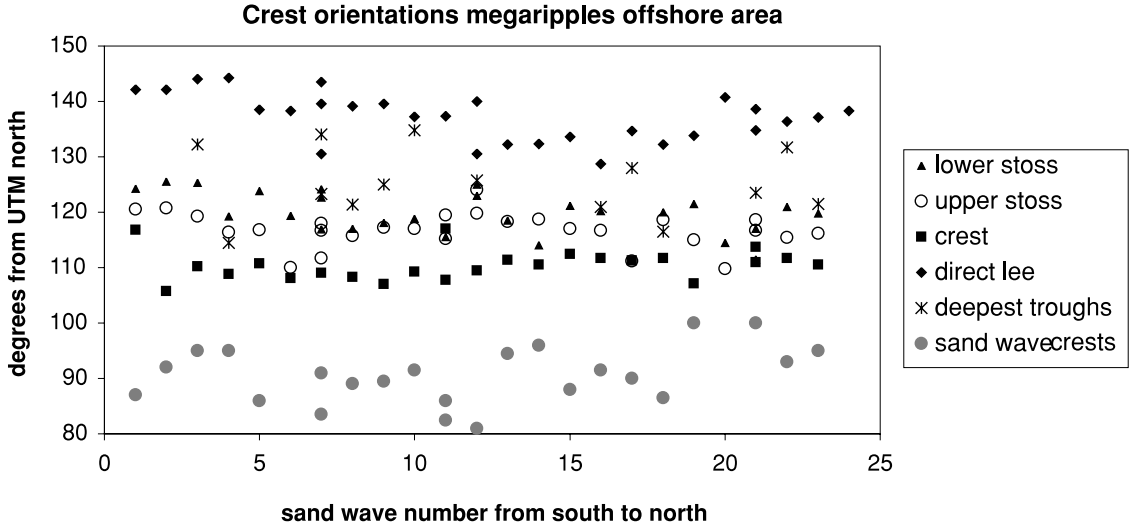

Figure 6. Crest orientations of megaripples (solid symbols) on different parts of the sand waves and sand waves (shaded symbol) in the offshore area, measured in September 2001. Sand waves 7 and 21 are bifurcated sand waves and were measured individually and plotted as one sand wave on the *x* axis.

wave troughs, megaripples are discontinuous and sinuous, showing enhanced backscatter in their wide troughs. On stoss slopes, megaripple crests are the most continuous and straight (2-D), with light acoustic shadows. Here, the average megaripple length is 10.14 m and heights are up to 0.40 m. Near sand wave crests, megaripple crests are straight 2-D and vague, or absent. With very few exceptions, megaripples are absent on lee slopes of the sharp-crested sand waves and are present on the lee slopes of rounded sand waves with lower slope angles.

[20] Plan view morphodynamics of compound sand waves in the offshore area indicate that sand waves are not significantly changed in pattern, size or appearance. Superimposed megaripples, on the other hand, vary in form from continuous and straight crested with wavelengths of approximately 7 m in March 2001, to strongly bifurcated megaripples with zigzag junctions and wavelengths of 7–10 m in June/July 2001 and April 2002. Straight 2-D megaripples with few zigzag junctions and wavelengths of approximately 2 m occurred in October 2001.

[21] The comparison of the March 2001 and April 2002 profiles in the offshore area reveals that the cross-sectional shapes of individual sand waves, too, remain similar (Figure 5a). The horizontal displacement (Figure 7) of upper lee slopes of individual sand waves varies between 3.8 m southward, which is in the direction of the subordinate ebb tidal current, and 5.0 m northward (with one exception of 10.0 m), which is in the direction of the dominant flood current. The horizontal displacement of the lower lee slopes is between 0.0 m and an exceptional 11.2 m northward (Figure 7). These values correspond to a migration rate of sand waves in the offshore area of 3.4 m yr^{-1} southward to 4.5 m yr^{-1} northward for upper lee slopes and 0.0 m yr^{-1} to 10.2 m yr^{-1} northward for lower lee slopes. Both the migration directions and the migration rates are consistent with the findings of *Besio et al.* [2004] as referred to earlier in

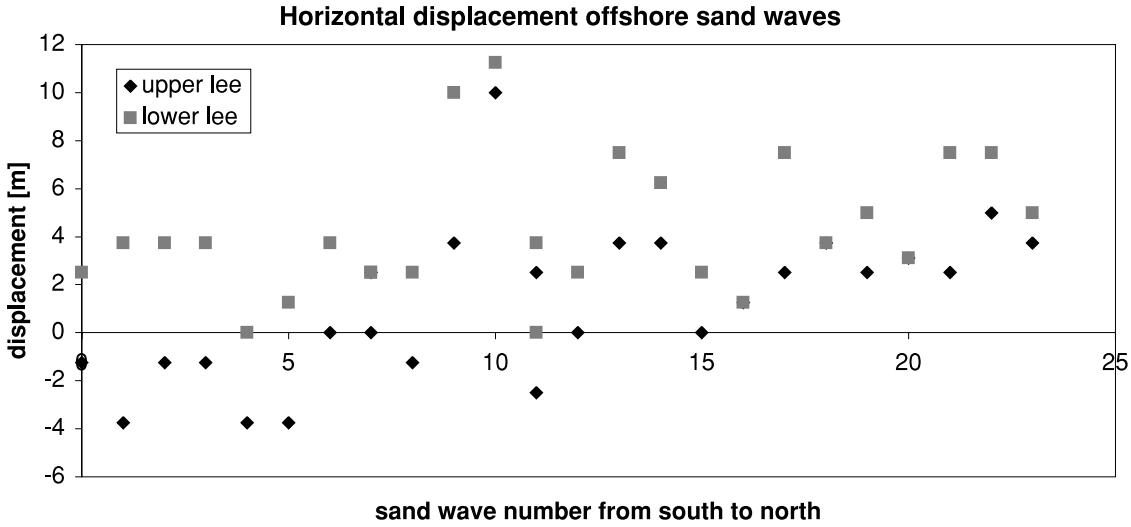

Figure 7. Migration distances of upper and lower lee slopes of individual sand waves in the offshore area between March 2001 and April 2002.

this paper. Our data of the offshore site are different from the data of *Lanckneus and De Moor* [1991] in that the sand waves they describe all migrate in the same direction at the same time and switch direction over time, whereas we find both southward and northward displacement of individual sand waves in the same period. The migration rates that we determined are smaller than those reported by *Lanckneus and De Moor* [1991].

[22] Seabed sediments in the offshore area are well-sorted, fine to coarse sands with grain sizes ranging between 150 and 700 μm and sample medians ranging between 254 and 304 μm (Table 1). Grains finer than 63 μm do not occur in the surface samples. Grain size distributions vary less between samples than in the coastal area. No fining or coarsening trends in the medians are apparent in the sampled area of this site. Grain size differences between sand wave crests and troughs are insignificant, on average 14 μm coarser at the crests, and are only systematic in June and September 2001 (see Passchier and Kleinhans, submitted manuscript, 2004, Figure 6)]. In comparison, *Tobias* [1989] reports differences in D50 between the sand wave crests and troughs of 52, 0, and 69 μm coarser at the crests of surveys near Platform Goeree and Eurogeul. We measured an average maximum seasonal variation of the medians per sample location of less than 18 μm, which is about the sampling error of ~20 μm.

4. Interpretation and Discussion

4.1. Relative Importance of Wave and Current Processes

[23] Sand wave saturation heights may reach one sixth of the water depth [*Yalin*, 1972] or 20% of the water depth when modeled in current-only conditions [*Németh and Hulscher*, 2003]. At our sites, sand wave heights are smaller. The continuous 2-D sand waves in the offshore area seem not restricted in their extent by either topography or water depth. The occurrence of the coastal 3-D sand waves, on the other hand, seems to be laterally limited to the shoreface-connected ridge and the flattening of sand waves in the coastal area implies vertical confinement by external factors, i.e., factors other than saturation. The contrast in sand wave morphology and migration rates at the two North Sea sites may be explained by the relative importance of surface waves and temporary or local current conditions. In shallow seas, tidal current bottom boundary layers are typically several to tens of meters thick, which is in the same order as the water depth [e.g., *Soulsby*, 1990, 1997; *Komarova and Hulscher*, 2000]. Surface waves in shallow waters may cause high orbital velocities at the bed, generating a wave bottom boundary layer, with a thickness in the order of centimeters. Since wave bottom boundary layers are much thinner than current boundary layers, they cause higher bed shear stresses for the same velocity values [*Fredsøe and Deigaard*, 1992; *Soulsby*, 1997], and are thus much more effective in mobilizing sediment.

[24] To account for the contrasting morphology of the bed forms at the two sites, the relative importance of current and wave processes on sediment mobility and morphology is determined by comparing dimensionless Shields mobility parameters for shear stress, θ, for both currents and waves, to their critical Shields parameters. Dimensionless Shields parameters are straightforwardly computed, when ignoring their different directions, by (Shields (1936) as discussed by *Van Rijn* [1993]):

$$\theta = \frac{\tau}{(\rho_s - \rho_w) g D_{50}} \tag{1}$$

in which the shear stress for currents is calculated by (White Colebrook equation discussed by *Van Rijn* [1993])

$$\tau = \rho_w g \left[\frac{u_c}{18^{10} \log\left(\frac{12h}{2.5 D_{50}}\right)} \right]^2 \tag{2}$$

and that for waves by (Swart (1976) discussed by *Van Rijn* [1993]):

$$\tau = \rho_w u_{orb}^2 \exp\left[5.213 \left(\frac{2.5 D_{50}}{A_{orb}}\right)^{0.194} - 5.977 \right] \tag{3}$$

[25] In the calculations of the dimensionless shear stress, we used measured significant wave heights and wave periods from monitoring stations at Noordwijk and IJmuiden Munition Dump, the nearest stations to respective the coastal and offshore site (Figures 8 and 9). We used averages of grain sizes of 300 μm at 14 and 17 m water depths and 275 μm at 25 and 30 m water depths (Table 1).

[26] For currents, the critical Shields parameter is only exceeded at current velocities larger than 0.4 m s^{-1} (Figure 10a). Near-bottom measurements of *Van de Meene* [1994] show that peak flood currents just south of the coastal area are 0.76 m s^{-1} during January/February 1991. Near-bottom tidal current measurements at the IJmuiden station from March 2001 are not available. Alternatively, in 2002, current measurements during quiet periods of low wind speeds, i.e., when wind-driven current enhancement is minimal, show that peak flood currents do not, and ebb currents only briefly exceed 0.4 m s^{-1} during neap tide (Figure 11). During spring tide, peak ebb currents are 0.6 m s^{-1} and peak flood currents are 0.8 m s^{-1}, with exceptions of more than 1.0 m s^{-1}, exceeding the critical velocity for 60% to 70% of the time. The direction of the tidal currents near the coast is forced to be longshore by the presence of the coast itself [*Van der Giessen et al.*, 1990]. At Noordwijk, coastal currents (NWK4) are strongly flood dominated during spring tide, with peak ebb currents around 0.4 m s^{-1} and peak flood currents up to 0.6 m s^{-1} (Figure 12). Velocities exceed the critical flow velocity for less than 20% of the time for spring ebb and 35% of the time for spring floods. During neap tide, neither ebb nor flood currents exceed the critical value of 0.4 m s^{-1} near the coast (Figure 12). *Van der Giessen et al.* [1990] analyzed this data set and found that current velocities increase with distance from the coast (see also Figure 12). Currents 30 km offshore west of Noordwijk are less strongly flood dominated and show peak ebb currents of 0.8 m s^{-1} and peak flood currents of 0.9 m s^{-1} during spring tide. For NWK 10, 20 and 30, current velocities during spring tides exceed the critical velocity 65% to 75% of the time. During neap tide, neither ebb nor flood currents exceed the critical value of 0.4 m s^{-1}. When applying these measurements to our sites,

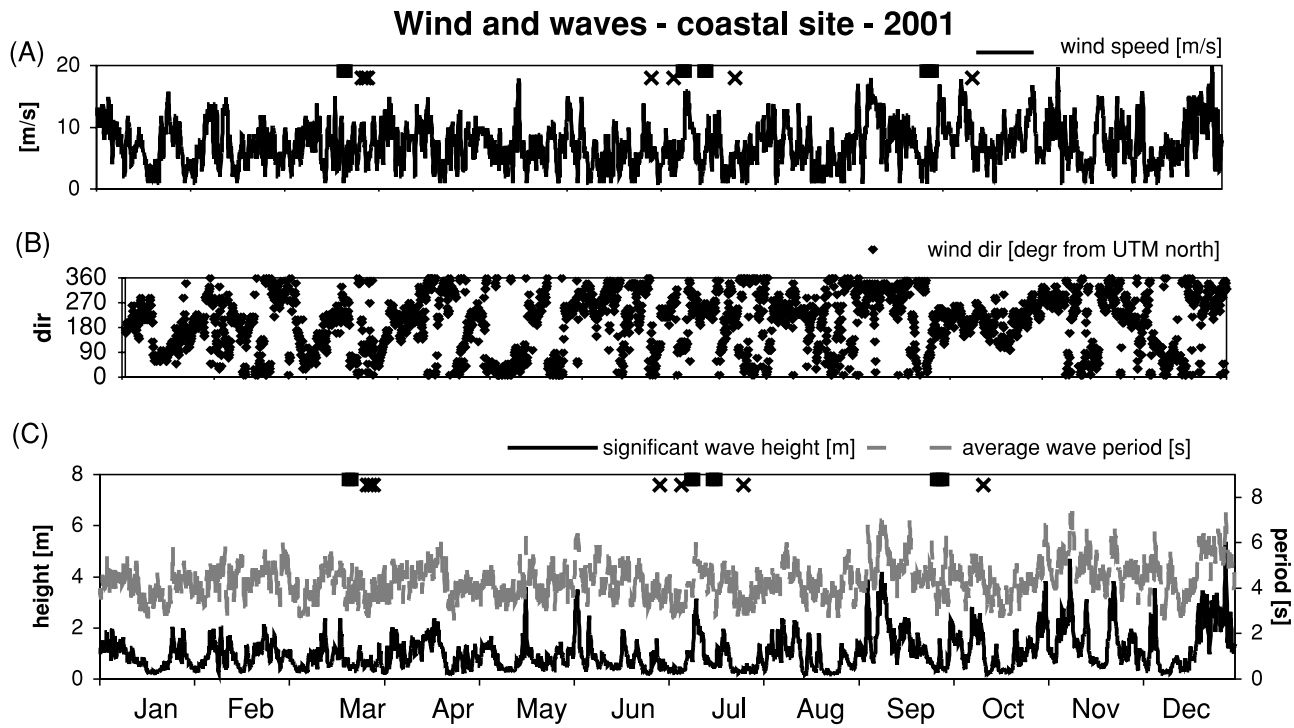

Figure 8. (a) Three-hourly averages of wind speed, (b) wind direction, and (c) significant wave height and wave period measured every 10 min at monitoring station Noordwijk (MPN) in 2001 (http://www.golfklimaat.nl). The period of data acquisition in the coastal area is indicated at the top of the plots by squares (multibeam) and crosses (side-scan sonar).

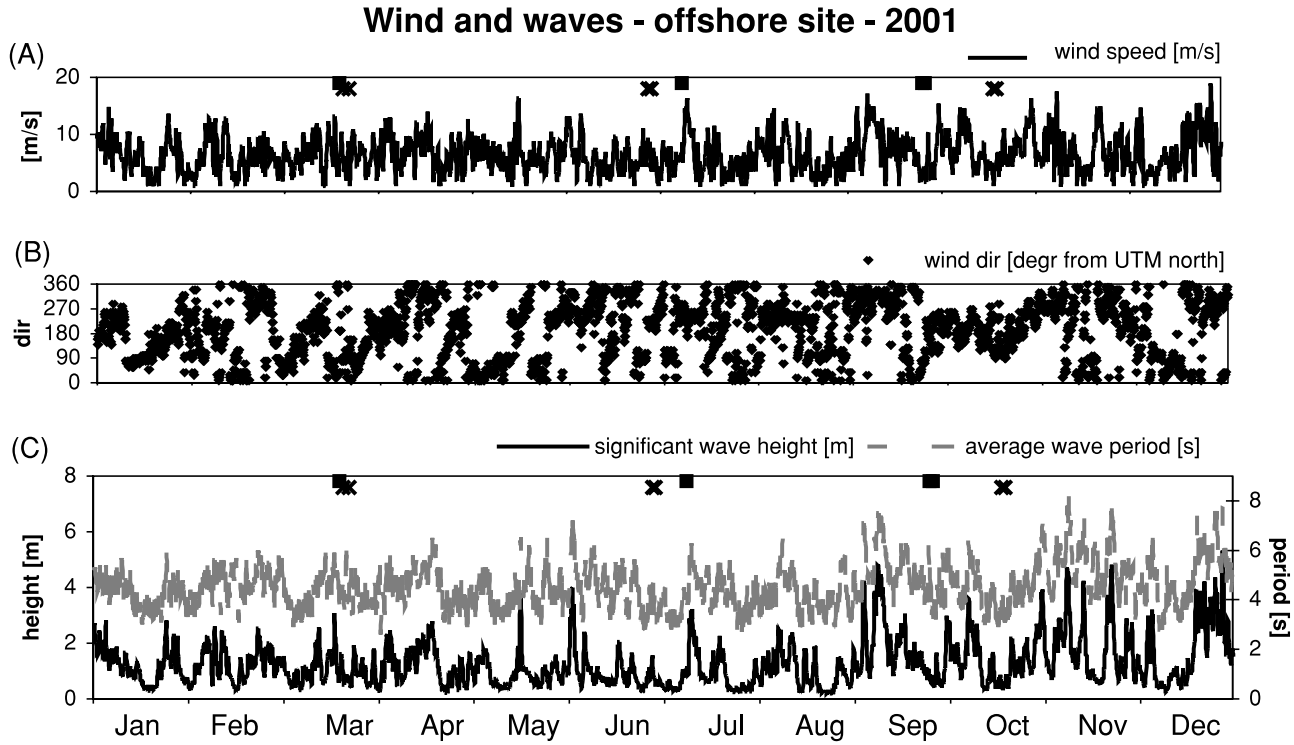

Figure 9. (a) Three-hourly averages of wind speed, (b) wind direction, and (c) significant wave height and wave period measured every 10 min at IJmuiden Munition Dump in 2001 (http://www.golfklimaat.nl). The period of data acquisition in the offshore area is indicated at the top of the plots by squares (multibeam) and crosses (side-scan sonar).

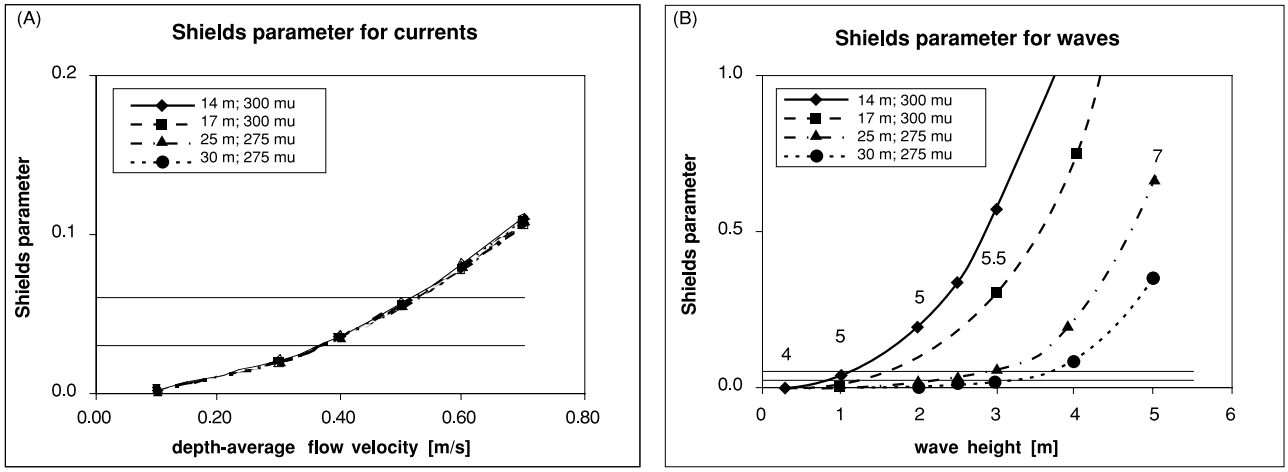

Figure 10. Shield parameter plots for (a) depth-averaged current velocity and (b) surface wave height at different water depths. Ranges of critical Shields parameters are indicated by the horizontal dashed lines. Grain sizes at water depths used in the calculations are realistic averages from field measurements. For waves (Figure 10b), wave periods are realistic averages measured at monitoring stations Noordwijk and IJmuiden Munition Dump.

currents are stronger and exceed the critical Shields parameter for longer periods in the offshore are than in the coastal area. Sediment mobility during current-only conditions is sufficient to change the seabed at both North Sea sites during ebb and flood spring tides, and near the coast only during spring floods, which is more than 50% of the time.

[27] For waves, significant wave heights of 1 m and periods of 5 s already exceed the threshold for motion at the bed at 14–17 m water depths (Figure 10b). At the coastal site, surface wave heights during fair weather conditions, such as in January to March 2001, are between 0.3 and 2.5 m (Figure 8) and cause Shields mobility parameters to exceed the critical value. From linear wave theory it was calculated that at the shallow coastal site, the orbital velocity at the bed is of the same order of magnitude as the tidal current velocity. At the offshore site, water depths are sufficiently large to reduce the magnitude and frequency of surface wave impact on the sand waves. Figure 10b

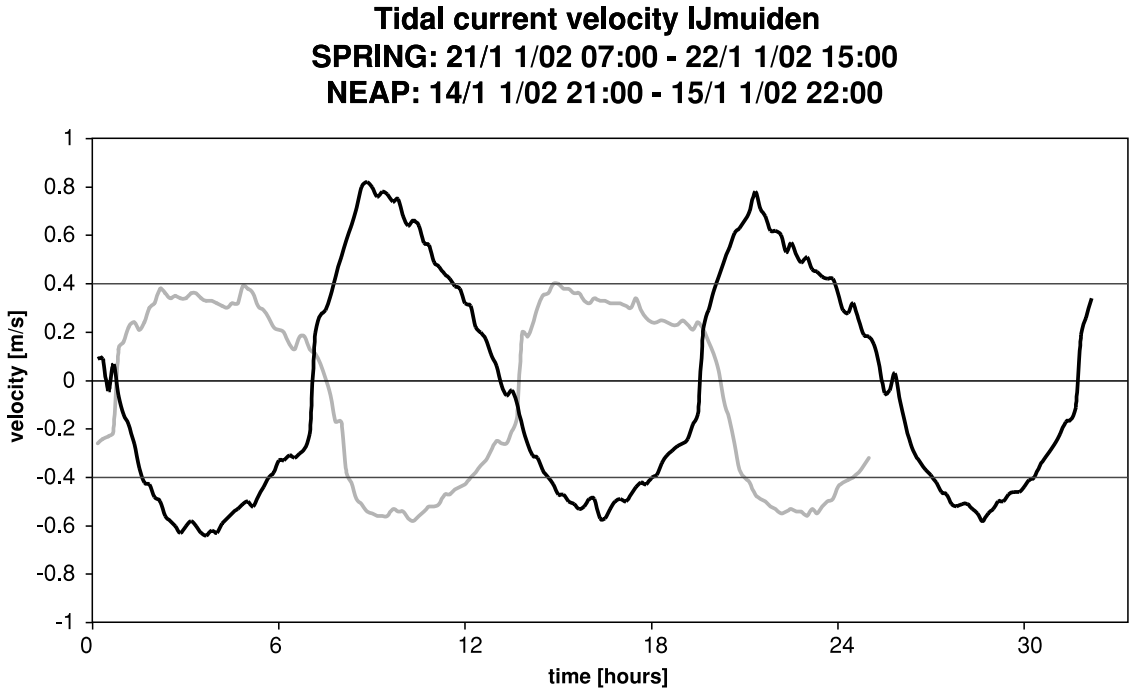

Figure 11. Tidal current velocities near the bed during quiet periods with wind speeds less than 8 m s^{-1} for both spring (solid line) and neap (shaded line) tides, measured at IJmuiden station (http://www.donarweb.nl). The critical velocity for current-only sand transport is indicated for ebb (negative) and flood (positive).

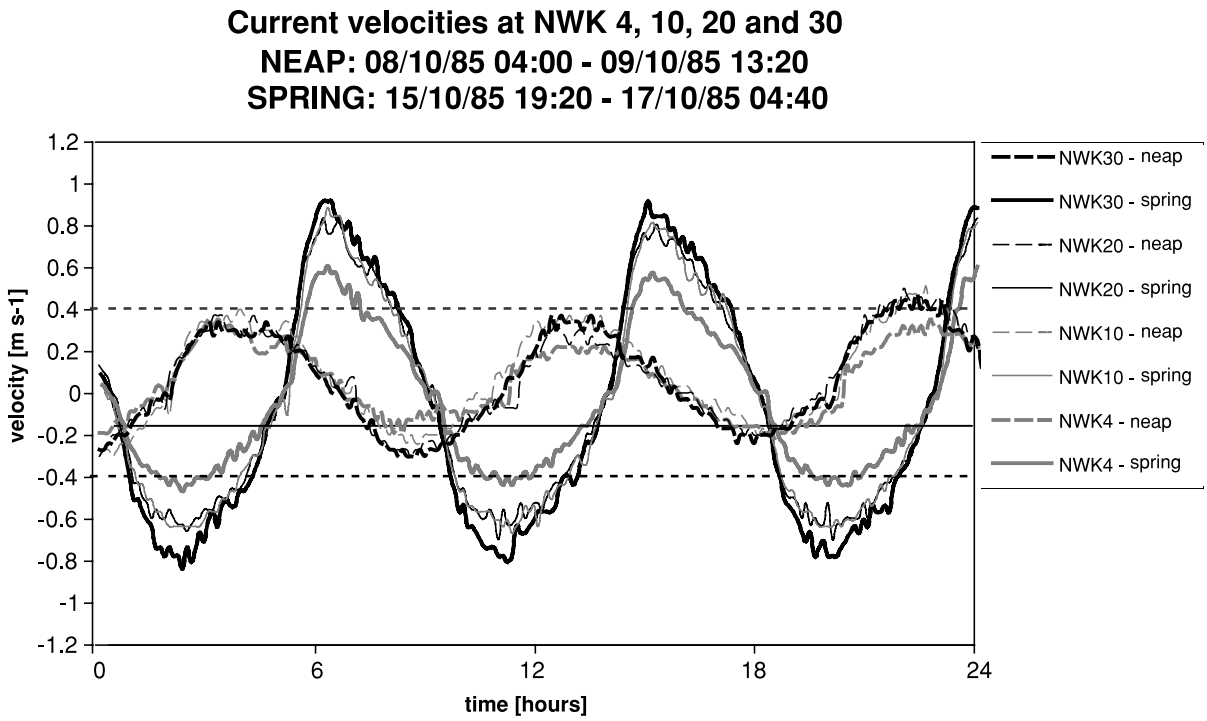

Figure 12. Tidal current velocities at 5 m above the bed during quiet periods with wind speeds less than 8 m s^{-1} for both spring (solid line) and neap (dashed line) tides, measured at stations 4, 10, 20 and 30 km offshore from Noordwijk (http://www.waterbase.nl; http://www.donarweb.nl). The critical velocity for current-only sand transport is indicated for ebb (negative) and flood (positive). For the correction of the critical velocity for velocity measurements at 5 m above the bed a hydraulic roughness has to be assumed. We therefore accept the marginal error in the interpretation and use the critical flow velocity as indicative. See color version of this figure in the HTML.

shows that only waves with wave heights larger than 3 m and wave periods of 5.5 s exceed the critical Shields parameter at 25 and 30 m water depths, which limits the effects of waves in the offshore site to only several events per year and excludes January to mid May 2001 (Figure 9).

[28] The measure of wave susceptibility of the bed and the duration of storms and quiet periods, explain the contrast in morphology and development of the compound sand waves. The above calculations and reported local conditions indicate that the coastal site is subject to significant wave action all year and that current velocities are only sufficient for sediment mobility during spring floods. In contrast, the offshore site experiences sufficient wave action only during major events and both ebb and flood current velocities are sufficient for sediment mobility at the bed during spring tide. Since wave action is subordinate at the offshore site, the sharp-crested sand waves are interpreted as current bed forms with occasional interaction of waves. Here, the sand wave heights are determined by saturation, a mechanism based on the balance between the bed shear stress and the effect of bed slope on the sediment transport [*Németh and Hulscher*, 2003]. Periods of current action versus wave and current interaction are indicated by the superimposed, straight 2-D asymmetrical megaripples in March 2001 versus the bifurcated asymmetrical megaripples in July and September 2001 and April 2002. The straight 2-D megaripples are interpreted as stable current bed forms that were restored during quiet periods after storms and bifurcated megaripples as transitional forms of short-lived instability [*Hansen et al.*, 2001]. In the coastal site, where the impact of waves is larger and wave and current interaction is more consistent, megaripples are obliterated and wave-generated hummocky bed forms are even formed (Passchier and Kleinhans, submitted manuscript, 2004). The obliteration of megaripples due to storms was earlier identified by *Tobias* [1989] and *Houthuys et al.* [1994]. Here compound sand waves are flattened by wave action in such a magnitude and frequency that they cannot be restored by the short-duration spring floods, and may not reach saturation. The laterally restricted 3-D sand waves on top of the shoreface-connected ridge and the continuous 2-D offshore sand waves correspond to the interpretation of an increased wave impact at the coastal site and the dominant current impact at the offshore site. The combined impact of currents and waves on beds at our coastal site is also supported by the interpretation of sedimentary structures made by *Van de Meene et al.* [1996].

[29] The absence of megaripples on lee slopes of sharp-crested compound sand waves was previously attributed to unidirectional currents with flow separation, while the presence of megaripples on the lee sides of rounded sand waves was attributed to bidirectional currents with unseparated flow [*Reading*, 1986, Figure 9.35]. However, flow separation does not occur at slope angles smaller than 10° to

14° [*Best et al.*, 2004; *Wilbers*, 2004]. We observed that megaripples are absent on lee slopes of sand waves with gradients larger than 1.8° and are present on slopes less than 2.1° in the offshore area. *Németh et al.* [2002, p. 2803] showed that the bed slope term, a factor which takes into account that sand is more easily transported downward than upward, (1) plays an important role in determining the fastest growing mode, which is the bed form of a certain wavelength that will be selected by the system, and (2) dampens the smaller bed forms, i.e., bed forms of small wavelengths are not formed when the bed slope is large. *Idier et al.* [2004] suggest that the apparent roughness related to the flow acceleration over a sand wave is dominant in the sharp increase and decrease of the bed shear stress over a sand wave, which causes the respective presence of megaripples on the stoss slopes and absence of megaripples on lee slopes. We interpreted that at a lee slope gradient of 2° is the empirical threshold, above which megaripples are absent.

[30] The angle between the crest orientations of sand waves and superimposed megaripples as observed in the offshore area is explained by the deflection of the tidal current over sand waves due to the Bernouilli effect, which is the deflection of the flow direction by current velocity variations over bottom undulations [*Terwindt*, 1971; *Malikides et al.*, 1989; *Hennings et al.*, 2000]. The implied deflection of the tidal current is confirmed by the systematic change of megaripple crest orientations over the length of a sand wave, as observed in the offshore area (Figure 6). Here megaripples near the sand wave crests are oriented approximately normal to the overall tidal current direction. The orientation of the sand wave crests, which is 10°–20° with respect to the overall tidal current direction, is explained by the anticlockwise veering of the currents in a vertical direction due to the Coriolis force (Ekman spiraling) [*Hulscher*, 1996]. In the coastal area, both sand wave and megaripple crests are oriented approximately normal to the surface tidal current of 19°, which latter is parallel to the coastline. The current deflection at this site seems minor with megaripple crest orientations on the stoss slopes of 103° and showing adjustment to the orientation of the sand wave crests when approaching these crests. Although less than in the offshore area, the large-scale morphology controls the orientation of the megaripples by deflecting the local flow.

[31] The different appearance and form of megaripples over the lengths of sand waves on sonograms suggests that not only flow direction is different but that the flow type or velocity also vary. These differences cannot be due to different ensonification angles of the side-scan sonar, since the sonar tracks were sailed in the migration direction of the sand waves. Recent ADCP measurements confirm that current velocities vary over the lengths of sand waves [*Hennings et al.*, 2004; *Kostaschuk et al.*, 2004].

[32] The hypothesis that sand waves are relic forms from former conditions [e.g., *Hennings et al.*, 2000] has been refuted by (1) their sharp-crested cross-sectional profiles, (2) the positive relation between upper/lower lee migration, (3) albeit slowly, they migrate (rates > 1 m yr^{-1}) and aggrade vertically and are thus contemporarily being developed, and (4) the formation and active development of smaller superimposed bed forms such as the bifucation and straightening of megaripple crests.

4.2. Sand Wave Migration

[33] The variable direction and rates of sand wave migration over time that we describe in this paper and that were earlier reported by *Lanckneus and De Moor* [1991] and *Besio et al.* [2004] suggest that measurements of sand wave dynamics are highly dependent on the period during which data were acquired, and thus seem coincidental. Long-term observations on the scale of years would indicate the validity of these shorter-term observations. Nevertheless, the variable dynamic behavior of compound sand waves between the coastal and offshore sites in the North Sea is evident by, for the coastal site, the high migration rates of sand waves and the surface wave-related obliteration of megaripples versus the low migration rates of sand waves and the survival of megaripples, which latter vary in surface expression for the offshore site. The different migration behavior of sand waves in the coastal and offshore areas is explained by two major factors. First, the contrast in bidirectional flow regime at the offshore site, where both ebb and flood currents are significant during spring tide, and the effectively unidirectional flow regime near the coast, where ebb currents are subordinate during both spring and neap tides and only spring floods can mobilize sediments. Second, the dominant current action in the offshore area and the consistent combined wave and current action in the coastal area results in larger net transport by tidal currents due to wave stirring in the coastal area, which increases the migration rates of the coastal sand waves [*Calvete et al.*, 2002].

[34] Sensitivity diagrams of Shields parameters (Figure 13) indicate that Shields parameters for waves are sensitive for grain size differences and changes in water depth, whereas those for currents depend on mostly grain size. Thus the behavior of current-maintained bed forms is controlled by changes in sediment mobility due to grain size, whereas the behavior of wave-maintained bed forms would be influenced by both grain size and water depth (more by water depth than grain size). This may already follow from equations (2) and (3). The additional value of the diagrams, however, is that despite the recently suggested control of grain size on bed form dimension [e.g., *Flemming*, 2000; *Bartholdy et al.*, 2002; *Németh et al.*, 2002; *Bartholdy et al.*, 2004], the diagrams show that the small differences in grain size between our coastal and offshore areas are not sufficient to cause major differences in sediment mobility. Water depth determines the current/wave dominancy of the local hydraulic regime, which supports that at our sites, wave stirring causes the large differences in the migration rate. This implies that in the combined current and wave regime of the coastal site, bed form dynamics are controlled by water depth whereas in the current-dominated regime of the offshore site, bed form dynamics are controlled by grain size.

5. Conclusions

[35] 1. The morphology and dynamics as determined from time records of multibeam and side-scan sonar imagery show that the coastal and offshore compound sand waves investigated in this paper are nonrelic forms that actively develop and migrate.

[36] 2. Wave action is significant in the coastal area and affects the morphology of the sand waves. Wave orbital

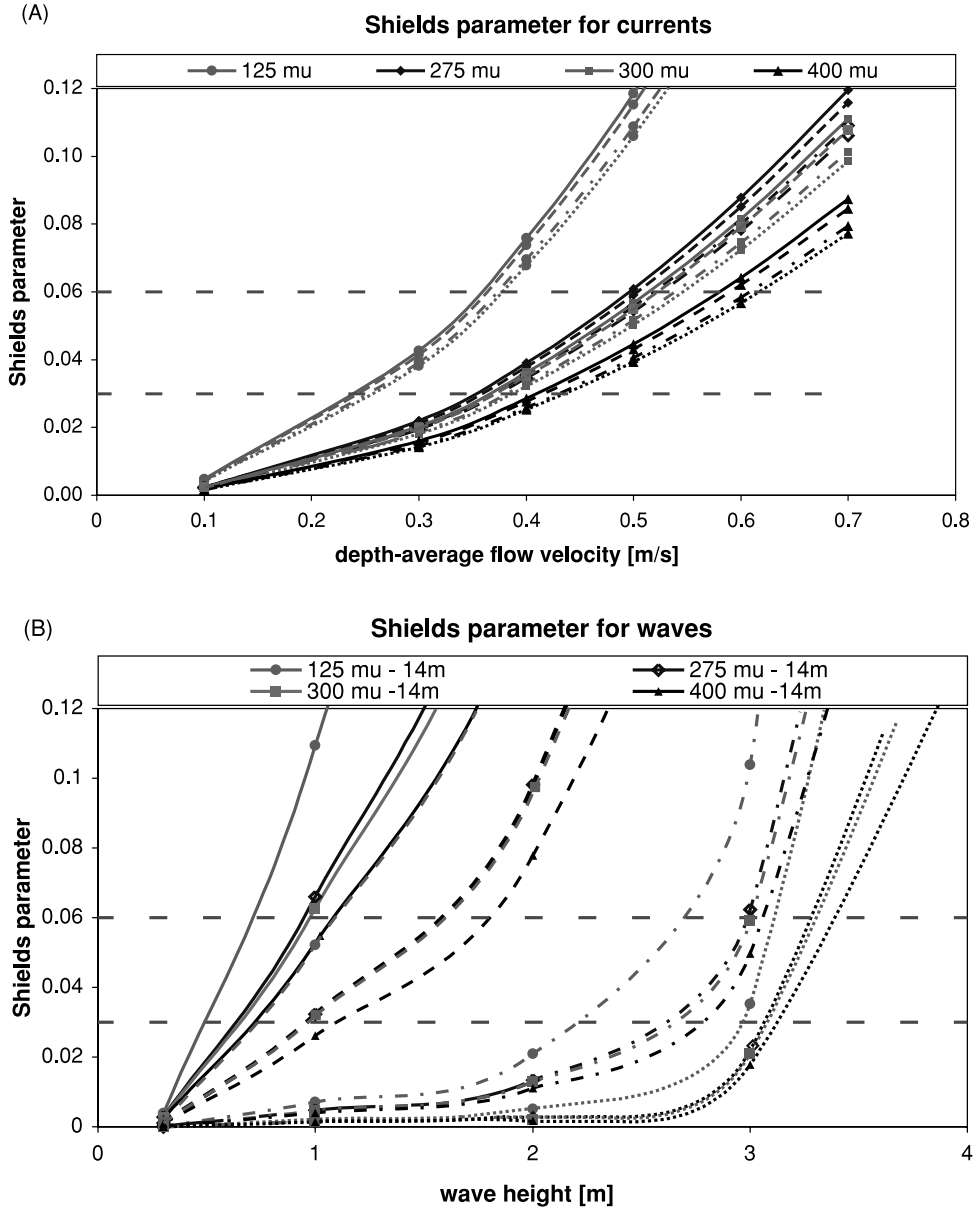

Figure 13. Sensitivity diagrams of Shields parameters for (a) currents and (b) waves. Grain sizes are indicated by node type: solid circles for 125 μm, open diamonds for 275 μm, solid squares for 300 μm, and solid triangles for 400 μm. Water depths are indicated by line type: solid line for 14 m, long-dashed line for 17 m, dashed-dotted line for 25 m, and dotted line for 30 m. See color version of this figure in the HTML.

motion at the bed is sufficient to stir up sand. The flattened sand waves in the coastal area result from the attenuation of sand waves caused by wave action in such a magnitude and frequency that they cannot be restored by the tidal current. Water depths in the offshore area are sufficient to reduce the impact of surface waves on the sand waves and to reduce the frequency of impact to several events per year, thereby allowing currents to be the major process in the development of compound sand waves.

[37] 3. The high migration rates of compound sand waves in the coastal area (6.5 to 20 m yr^{-1}) are caused by the interaction of wave stirring and flood-dominated longshore currents. In the offshore area, where the behavior of compound sand waves is controlled by the current regime and wave stirring does nor occur, migration rates are low (-3.6 to 10 m yr^{-1}).

[38] 4. Sediment grain size controls the sediment mobility in current-dominated regimes and is subordinate to water depth in wave-dominated regimes. The small grain size differences in the coastal and offshore areas in this study are not sufficient to cause differences in the migration rate.

[39] 5. The occurrence of megaripples is directly related to lee slope gradients of the sand waves. The threshold of lee slope gradients is 2°, above which megaripples are absent.

[40] 6. The variable orientations of megaripples over the length of a sand wave are explained by the deflection of the

local flow by the large-scale morphology of sand waves. This effect is largest in the offshore area, where sand waves are relatively steep, and smaller in the coastal area. However, the angle between the sand wave and megaripple crests in the offshore area versus the parallelism of these in the coastal area remains unexplained. The different appearance of the megaripples over the lengths of sand waves corresponds to variations in current velocity over the lengths of sand waves found elsewhere.

[41] 7. Wave action during near gales, gales and storms remold or obliterate the superimposed megaripples on the sand waves, whereas maximum tidal currents under fair weather conditions allow superimposed megaripples on the sand waves to be formed.

Notation

θ	dimensionless Shields mobility parameter.
τ	shear stress, N m^{-2}.
ρ_s	specific weight of sediment, g L^{-1}.
ρ_w	specific weight of water, g L^{-1}.
g	gravitational acceleration, 9.81 m s^{-2}.
D_{50}	local median sediment diameter, m.
u_c	tidal current velocity, m s^{-1}.
h	local water depth, m.
u_{orb}	significant orbital velocity, m s^{-1}.
A_{orb}	orbital diameter from linear theory, m.
H_{sig}	significant wave height, m.
T_p	wave period, s.

[42] **Acknowledgments.** Data were collected by S. Passchier (TNO-NITG) in collaboration with the Directorate North Sea, Dutch Public Works and Water Management (DNZ-RWS) aboard the Ms. *Arca* of DNZ-RWS. S. Bicknese (DNZ-RWS) and J. Doekes (RIKZ-RWS) are acknowledged for providing digital multibeam and current velocity data. R. Savert (TNO-NITG) drew most of the figures. This work was part of the project "Eco-morphodynamics of the seafloor," financed by Delft Cluster, the project "Dynamics and sediment classification of the North Sea bed" (DYSC) of the Netherlands Institute of Applied Geosciences (TNO-NITG), and the EU SANDPIT project (MAS3-CT97-0086). This work will contribute to the MESH project (Mapping European Seabed Habitats, http://www.searchmesh.net) and received European Regional Development Funding through the INTERREG III B Community Initiative (http://www.nweurope.org). This paper was much improved thanks to the reviewers' comments.

References

Ashley, G. M. (1990), Classification of large-scale subaqueous bedforms: A new look on an old problem, *J. Sediment. Petrol.*, *60*(1), 160–172.

Bartholdy, J., A. Bartholomae, and B. W. Flemming (2002), Grain-size control of large compound flow-traverse bedforms in a tidal inlet of the Danish Wadden Sea, *Mar. Geol.*, *188*(3), 391–413.

Bartholdy, J., B. W. Flemming, A. Bartholomae, and V. B. Ernstsen (2004), On the dimensions of depth-dependent, simple subaqueous dunes, in *Marine Sandwave and River Dune Dynamics*, edited by S. J. M. H. Hulscher, T. Garlan, and D. Idier, pp. 9–16, Univ. of Twente, Enschede, Netherlands.

Besio, G., P. Blondeaux, M. Brocchini, and G. Vittori (2003), Migrating sand waves, *Ocean Dyn*, *53*, 232–238, doi:10.1007/s10236-003-0043-x.

Besio, G., P. Blondeaux, M. Brochinni, and G. Vittori (2004), On the modeling of sand wave migration, *J. Geophys. Res.*, *109*, C04018, doi:10.1029/2002JC001622.

Best, J., R. Kostaschuk, and R. Hardy (2004), The fluid dynamics of low-angle river dunes: Results from integrated field monitoring, laboratory experimentation and numerical modelling, in *Marine Sandwave and River Dune Dynamics*, edited by S. J. M. H. Hulscher, T. Garlan, and D. Idier, pp. 17–23, Univ. of Twente, Enschede, Netherlands.

Blondeaux, P., and G. Vittori (1999), Boundary layer and sediment dynamics under sea waves, *Adv. Coastal Ocean Eng.*, *4*, 133–191.

Blondeaux, P., M. Brocchini, and G. Vittori (2000), A model for sand waves generation, in *Proceedings of the First International Workshop on Marine Sandwave Dynamics*, edited by A. Trentesaux and T. Garlan, pp. 29–35, Univ. of Lille, Lille, France.

Calvete, D., H. E. de Swart, and A. Falqués (2002), Effect of depth-dependent wave stirring on the final amplitude of shoreface-connected sand ridges, *Cont. Shelf Res.*, *22*, 2763–2776.

Davies, A. G., L. C. Van Rijn, J. S. Damgaard, J. Van de Graaff, and J. S. Ribberink (2002), Intercomparison of research and practical sand transport models, *Coastal Eng.*, *46*, 1–23.

Flemming, B. W. (2000), The role of grain size, water depth and flow velocity as scaling factors controlling the size of subaqueous dunes, in *Proceedings of the First International Workshop on Marine Sandwave Dynamics*, edited by A. Trentesaux and T. Garlan, pp. 55–60, Univ. of Lille, Lille, France.

Fredsøe, J., and R. Deigaard (1992), *Mechanics of Coastal Sediment Transport*, 369 pp., World Sci., Hackensack, N. J.

Hansen, J. L., M. van Hecke, A. Haaning, C. Ellegaard, K. H. Andersen, T. Bohr, and T. Sams (2001), Instabilities in sand ripples, *Nature*, *410*, 324.

Hennings, I., B. Lurin, C. Vernemmen, and U. Vanhessche (2000), On the behaviour of tidal current direction due to the presence of submarine sand waves, *Mar. Geol.*, *169*, 57–68.

Hennings, I., D. Herbers, K. Prinz, and F. Ziemer (2004), On waterspouts related to marine sandwaves, in *Marine Sandwave and River Dune Dynamics*, edited by S. J. M. H. Hulscher, T. Garlan, and D. Idier, pp. 88–95, Univ. of Twente, Enschede, Netherlands.

Houthuys, R., A. Trentesaux, and P. De Wolf (1994), Storm influences on a tidal sandbank's surface (Middelkerke Bank, southern North Sea), *Mar. Geol.*, *121*, 23–41.

Hulscher, S. J. M. H. (1996), Tidal-induced large-scale regular bed form patterns in a three-dimensional shallow water model, *J. Geophys. Res.*, *101*(C9), 20,727–20,744.

Hulscher, S. J. M. H., and G. M. Van den Brink (2001), Comparison between predicted and observed sand waves and sand banks in the North Sea, *J. Geophys. Res.*, *106*(C5), 9327–9338.

Idier, D., and D. Astruc (2003), Analytical and numerical modeling of sandbanks dynamics, *J. Geophys. Res.*, *108*(C3), 3060, doi:10.1029/2001JC001205.

Idier, D., D. Astruc, and S. J. M. H. Hulscher (2004), Influence of bed roughness on dune and megaripple generation, *Geophys. Res. Lett.*, *31*, L13214, doi:10.1029/2004GL019969.

Komarova, N. L., and S. J. M. H. Hulscher (2000), Linear instability mechanisms for sand wave formation, *J. Fluid Mech.*, *413*, 219–246.

Kostaschuk, R., J. Blair, P. Villard, and J. Best (2004), Morphological response of estuarine subtidal dunes to flow over a semidiurnal tidal cycle: Fraser River, Canada, in *Marine Sandwave and River Dune Dynamics*, edited by S. J. M. H. Hulscher, T. Garlan, and D. Idier, pp. 160–167, Univ. of Twente, Enschede, Netherlands.

Lanckneus, J., and G. De Moor (1991), Present-day evolution of sand waves on a sandy shelf bank, *Oceanol. Acta*, *SP-11*, 123–127.

Malikides, M., P. T. Harris, and P. M. Tate (1989), Sediment transport and flow over sandwaves in a non-rectilinear tidal environment: Bass Strait, Australia, *Cont. Shelf Res.*, *9*(3), 203–221.

Németh, A. A. (2003), Modelling offshore sand waves, Ph.D. thesis, 140 pp., Univ. of Twente, Enschede, Netherlands.

Németh, A. A., and S. J. M. H. Hulscher (2003), Finite amplitude sand waves in shallow seas, in *IAHR Symposium on River, Coastal and Estuarine Morphodynamics*, edited by S. Sánchez-Arcilla and A. Bateman, pp. 435–444, Univ. Politec. de Catalunya, Barcelona, Spain.

Németh, A. A., S. J. M. H. Hulscher, and H. J. de Vriend (2002), Modelling sand wave migration in shallow shelf seas, *Cont. Shelf Res.*, *22*, 2795–2806.

Reading, H. G. (1986), *Sedimentary Environments and Facies*, 615 pp., Blackwell, Malden, Mass.

Soulsby, R. L. (1990), Tidal-current boundary layers, in *The Sea*, vol. 9, *Ocean Engineering Science*, edited by B. Le Méhauté and D. M. Hanes, pp. 523–566, John Wiley, Hoboken, N. J.

Soulsby, R. L. (1997), *Dynamics of Marine Sands*, 249 pp., Thomas Telford, London.

Terwindt, J. H. J. (1971), Sand waves in the Southern Bight of the North Sea, *Mar. Geol.*, *10*, 51–67.

Tobias, F. C. (1989), Morphology of sand waves in relation to current, sediment and wave data along the Eurogeul, North Sea, 60 pp., *Rep. GEOPRO 1989.01*, Dep. of Phys. Geogr., Univ. of Utrecht, Utrecht, Netherlands.

Trentesaux, A., A. Stolk, B. Tessier, and H. Chamley (1994), Surficial sedimentology of the Middelkerke Bank (southern North Sea), *Mar. Geol.*, *121*, 43–55.

Van Alphen, J. S. L. J., and M. A. Damoiseaux (1989), A geomorphological map of the Dutch shoreface and adjacent part of the continental shelf, *Geol. Mijnbouw*, *68*(4), 433–443.

Van de Meene, J. W. H. (1994), The shoreface-connected ridges along the central Dutch coast, Ph.D. thesis, 222 pp., Univ. of Utrecht, Utrecht, Netherlands.

Van de Meene, J. W. H., J. R. Boersma, and J. H. J. Terwindt (1996), Sedimentary structures of combined flow deposits from the shoreface-connected ridges along the central Dutch coast, *Mar. Geol.*, *131*, 151–175.

Van der Giessen, A., W. P. M. De Ruijter, and J. C. Borst (1990), Three-dimensional current structure in the Dutch coastal zone, *Neth. J. Sea Res.*, *25*(1–2), 45–55.

Van Rijn, L. C. (1993), *Principles of Sediment Transport in Rivers, Estuaries and Coastal Seas*, Aqua, Amsterdam.

Wilbers, A. (2004), The development and hydraulic roughness of subaqueous dunes, Ph.D. thesis, 227 pp., Utrecht Univ., Utrecht, Netherlands.

Yalin, M. S. (1972), *Mechanics of Sediment Transport*, Elsevier, New York.

M. G. Kleinhans, Department of Physical Geography, Institute of Marine and Atmospheric Research, University of Utrecht, P.O. Box 80115, 3508 TC Utrecht, Netherlands.

T. A. G. P. van Dijk, Netherlands Institute of Applied Geosciences, P.O. Box 80015, 3508 TA Utrecht, Netherlands. (t.vandijk@nitg.tno.nl)